

Diffractive ϕ -meson photoproduction on the proton near threshold

T. Mibe,^{1,2,*} W.C. Chang,³ T. Nakano,¹ D.S. Ahn,^{1,4} J.K. Ahn,⁴ H. Akimune,⁵ Y. Asano,⁶ S. Date,⁷ H. Ejiri,^{1,7} H. Fujimura,^{8,†} M. Fujiwara,^{1,9} K. Hicks,¹⁰ T. Hotta,¹ K. Imai,¹¹ T. Ishikawa,^{11,‡} T. Iwata,¹² H. Kawai,¹³ Z.Y. Kim,⁸ K. Kino,^{1,§} H. Kohri,¹ N. Kumagai,⁷ S. Makino,¹⁴ T. Matsuda,¹⁵ T. Matsumura,^{1,2,¶} N. Matsuoka,¹ K. Miwa,¹¹ M. Miyabe,¹¹ Y. Miyachi,^{16,**} M. Morita,¹ N. Muramatsu,¹ M. Niyama,¹¹ M. Nomachi,¹⁷ Y. Ohashi,⁷ T. Ooba,¹³ H. Ohkuma,⁷ D.S. Oshuev,³ C. Rangacharyulu,¹⁸ A. Sakaguchi,¹⁷ T. Sasaki,¹¹ P.M. Shagin,^{1,††} Y. Shiino,¹³ H. Shimizu,¹⁹ Y. Sugaya,^{17,2} M. Sumihama,^{17,2,‡‡} A.I. Titov,^{9,§§} Y. Toi,¹⁵ H. Toyokawa,⁷ A. Wakai,^{20,¶¶} C.W. Wang,³ S.C. Wang,^{3,***} K. Yonehara,^{5,†††} T. Yorita,⁷ M. Yoshimura,²¹ M. Yosoi,^{11,‡‡‡} and R.G.T. Zegers^{1,§§§}

(The LEPS collaboration)

¹Research Center for Nuclear Physics, Osaka University, Ibaraki, Osaka 567-0047, Japan

²Advanced Science Research Center, Japan Atomic Energy Research Institute, Tokai, Ibaraki 319-1195, Japan

³Institute of Physics, Academia Sinica, Taipei 11529, Taiwan

⁴Department of Physics, Pusan National University, Busan 609-735, Korea

⁵Department of Physics, Konan University, Kobe, Hyogo 658-8501, Japan

⁶Synchrotron Radiation Research Center, Japan Atomic Energy Research Institute, Mikazuki, Hyogo 679-5198, Japan

⁷Japan Synchrotron Radiation Research Institute, Mikazuki, Hyogo 679-5198, Japan

⁸School of Physics, Seoul National University, Seoul, 151-747, Korea

⁹Advanced Photon Research Center, Japan Atomic Energy Research Institute, Kizu, Kyoto, 619-0215, Japan

¹⁰Department of Physics and Astronomy, Ohio University, Athens, Ohio 45701, USA

¹¹Department of Physics, Kyoto University, Kyoto 606-8502, Japan

¹²Department of Physics, Yamagata University, Yamagata 990-8560, Japan

¹³Department of Physics, Chiba University, Chiba 263-8522, Japan

¹⁴Wakayama Medical University, Wakayama, 641-8509, Japan

¹⁵Department of Applied Physics, Miyazaki University, Miyazaki 889-2192, Japan

¹⁶Department of Physics and Astrophysics, Nagoya University, Nagoya, Aichi 464-8602, Japan

¹⁷Department of Physics, Osaka University, Toyonaka, Osaka 560-0043, Japan

¹⁸Department of Physics and Engineering Physics,

University of Saskatchewan, Saskatoon, Saskatchewan, Canada, S7N 5E2

¹⁹Laboratory of Nuclear Science, Tohoku University, Sendai, Miyagi 982-0826, Japan

²⁰Center for Integrated Research in Science and Engineering,

Nagoya University, Nagoya, Aichi 464-8603, Japan

²¹Institute for Protein Research, Osaka University, Suita, Osaka 565-0871, Japan

(Dated: August 12, 2005)

Photoproduction of ϕ -meson on protons was studied by means of linearly polarized photons at forward angles in the low-energy region from threshold to $E_\gamma = 2.37$ GeV. The differential cross sections at $t = -|t|_{min}$ do not increase smoothly as E_γ increases, but show a local maximum at around 2.0 GeV. The angular distributions demonstrate that ϕ -mesons are photo-produced predominantly by helicity-conserving processes, and the local maximum is not likely due to unnatural-parity processes.

PACS numbers: 13.60.Le, 25.20.Lj

The gluonic aspect of quantum chromodynamics (QCD), especially glueballs, has been of wide interest in hadron physics. It has been suggested that there is a connection between the glueball Regge trajectory ($J^{PC} = 2^{++}, 4^{++}, \dots$) and the Pomeron trajectory [1]. The diffractive photoproduction of ϕ -mesons has traditionally been used to study the Pomeron exchange process [2]. This is because the baryon and meson exchange amplitudes in the s- and t-channels are suppressed by the Okubo-Zweig-Iizuka (OZI) rule. Photoproduction of ϕ -meson is useful to study not only Pomeron exchange, but also other hadronic interactions mediated by multi-gluon exchanges which are difficult to identify in the other hadronic reactions due to large contributions from

baryon and meson exchanges.

The low-energy diffractive photoproduction of ϕ -mesons was suggested [3, 4] to be sensitive to a daughter Pomeron trajectory associated with a glueball ($J^{PC} = 0^{++}$) [3, 4, 5, 6]. Its contribution is expected to decrease rapidly with an increase of photon energy, whereas the contribution from Pomeron exchange increases. This difference may lead to a non-monotonic energy dependence of the forward-angle cross section near threshold ($E_\gamma = 1.57$ GeV). The existing cross section data in the low-energy region [7, 8, 9, 10, 11, 12] are still too poor to ascertain a possible signature of such a non-monotonic behavior.

The background contributions from s- and u-channels

diagrams, such as direct ϕ radiation from the nucleon [4, 13] and production in nucleon resonance decay [14, 15], are predicted to be small at small $|t|$ ($t = (p_\phi - p_\gamma)^2$). However, the contributions from the t -channel exchanges of pseudoscalar mesons (π, η), scalar mesons (f_0, a_0) [4, 16] and a tensor f_2' meson [17] are predicted not to be negligible. The energy dependence of those meson-exchange processes is expected to be similar to that of the daughter Pomeron trajectory. Therefore, to determine the relative contributions of these processes, we need to analyze the spin observables using linearly polarized photons.

The spin observables are studied via the decay angular distribution of the ϕ -meson in the K^+K^- decay mode. The decay angular distribution $W(\cos\theta, \phi, \Phi)$ is a function of the spin density matrix elements [18], where θ and ϕ denote the polar and azimuthal angles of the K^+ in the ϕ -meson rest frame. The azimuthal angle of the photon polarization in the center-of-mass frame is denoted by Φ . The relative contribution of natural-parity exchange and unnatural-parity exchange is related to the density matrix element $\bar{\rho}_{1-1}^1 (\equiv 1/2(\rho_{1-1}^1 - \text{Im}\rho_{1-1}^2))$ which is extracted from the one-dimensional distribution $W(\phi - \Phi)$ [15] through

$$W(\phi - \Phi) = \frac{1}{2\pi}(1 + 2P_\gamma \bar{\rho}_{1-1}^1 \cos 2(\phi - \Phi)), \quad (1)$$

where P_γ is the polarization of the photon beam. The available data at $E_\gamma = 2.8, 4.7, 9.3$ GeV [7] and 20-40 GeV [19] support the dominance of the helicity-conserving natural-parity exchange processes. However, there is no measurement of polarization observables near the threshold.

The decay angular distributions also provide information on helicity non-conserving processes. Recent measurements at low energies with unpolarized photons suggest significant contributions from the helicity non-conserving processes at large momentum transfer t [12, 20]. The contribution from helicity non-conserving mechanisms is examined by a deviation from the $\sin^2\theta$ behavior in the one dimensional distribution $W(\cos\theta)$ and an oscillation in the one dimensional distributions $W(\phi + \Phi)$, $W(\phi)$ and $W(\Phi)$.

In this Letter, we report measurements of the differential cross sections ($d\sigma/dt$) at small $|t|$ and the first measurements of decay angular distributions near threshold with linearly polarized photons. Linearly polarized photons were produced by means of the backward-Compton scattering of laser photons off the 8 GeV electron at the SPring-8 BL33LEP beamline (LEPS: Laser Electron Photons at SPring-8 facility) [21]. The maximum energy of the photon beam was 2.4 GeV. The photon energy was determined by measuring recoil electrons using a tagging counter with a resolution (σ) of 15 MeV. The typical photon flux was about 10^6 s^{-1} , which was monitored by counting scattered electrons with the tagging system.

The systematic uncertainty in the photon flux measurement was estimated to be 3%. The degree of linear polarization varied with photon energy; it was 95 % at the maximum energy, 60 % at 1.57 GeV. A liquid hydrogen target with a length of 50 mm was used in the experiment. A similar experiment with nuclear targets and the associated analysis have been reported in Ref. [22].

The momenta and the time-of-flight (TOF) of produced charged particles were measured with a magnetic spectrometer [21]. The angular coverage of the spectrometer is about ± 0.4 rad and ± 0.2 rad in the horizontal and vertical directions, respectively. The momentum resolution (σ) for 1 GeV/c particles was 6 MeV/c. The TOF resolution (σ) was 150 psec for a typical flight path length of 4 m. The mass resolution (σ) was 30 MeV/c² for a 1 GeV/c² kaon. Pions with momenta higher than 0.6 GeV/c and e^+e^- pairs were rejected by using an aerogel Cherenkov counter in the trigger level. An over-veto rate in the trigger was estimated to be less than 2.1%.

The incident photon energy and the momenta of K^+K^- tracks or $K^\pm p$ tracks were measured to identify the reaction $\gamma p \rightarrow K^+K^-p$ followed by the $\phi \rightarrow K^+K^-$ decay. Based on the detected particles, we define two types of event topology: K^+K^- -reconstructed events (KK mode), and $K^\pm p$ -reconstructed events (Kp mode).

The missing mass distribution for the $p(\gamma, K^+K^-)X$ reaction (denoted as $MM(\gamma, K^+K^-)$) is shown in

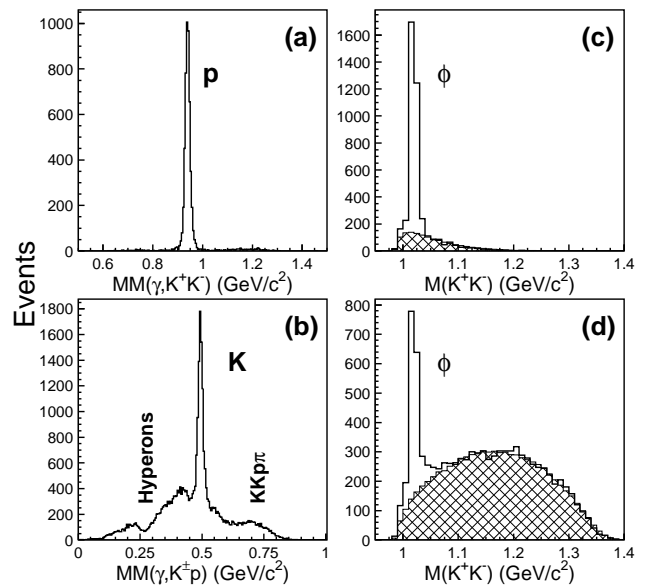


FIG. 1: (a) Missing mass distribution for the $p(\gamma, K^+K^-)X$ reaction in KK mode, (b) Missing mass distribution for the $p(\gamma, K^\pm p)X$ reaction in Kp mode. (c) and (d) are the K^+K^- invariant mass distributions after the cut on the missing mass for KK and Kp modes, respectively. The hatched histograms are the simulated background.

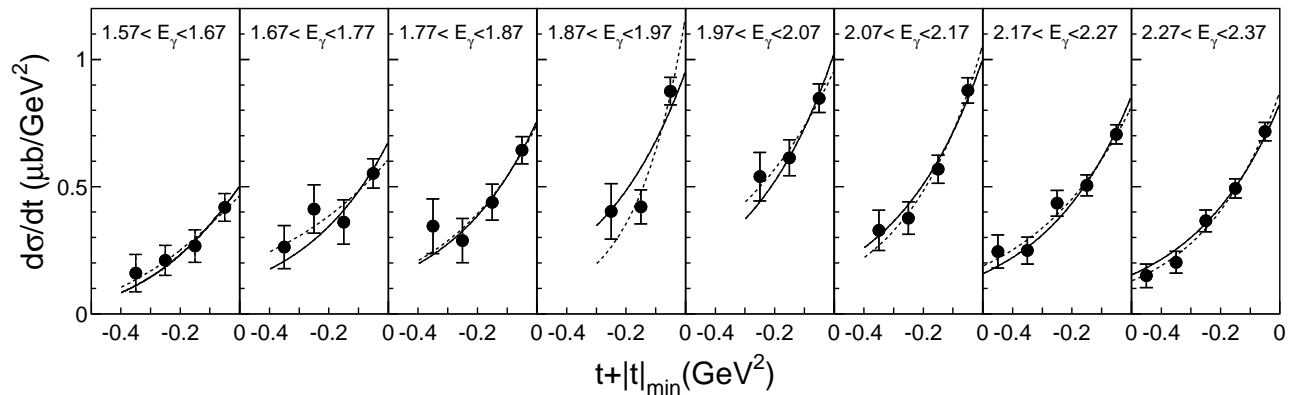


FIG. 2: Differential cross sections for the $\gamma p \rightarrow \phi p$ reaction. The dashed curves are the results of the fit using an exponential function $((d\sigma/dt)_{t=-|t|_{min}} e^{b(t+|t|_{min})})$ with $(d\sigma/dt)_{t=-|t|_{min}}$ and b as free parameters. The solid curves are fitted results with fixing $b = 3.38 \text{ GeV}^{-2}$. The error bars represent statistical errors. The systematic errors are discussed in the text.

Fig. 1(a) for KK mode. A sharp peak corresponding to the proton was observed with an average mass resolution (σ) of $10 \text{ MeV}/c^2$. The missing mass distribution for the $p(\gamma, K^\pm p)X$ reaction ($MM(\gamma, K^\pm p)$) is shown in Fig. 1(b) for Kp mode. A clear peak at the kaon mass was observed with an average mass resolution (σ) of $10 \text{ MeV}/c^2$. In Kp mode, there were contributions from non- K^+K^-p final states. The background below the kaon peak is attributed mainly to hyperon photoproduction having a non- K^+K^-p final state, such as $Kp\pi\gamma$, $Kp\pi\pi$. The background above the kaon peak is due to $KKp\pi$ events. A 3σ cut on the missing mass spectrum was applied to select the K^+K^-p final state.

Figure 1(c) and (d) show the K^+K^- invariant mass distributions for KK and Kp modes, respectively. In Kp mode, the momentum of the missing kaon was calculated by assuming a K^+K^-p final state. The cut point on the K^+K^- invariant mass was set to $1.009 < M(K^+K^-) < 1.029 \text{ GeV}/c^2$ which corresponded to about 10 % loss of ϕ events. The background in the ϕ peak region was estimated with the following method. We considered two sources of background; photoproduction of $\Lambda(1520)$ and a K^+K^-p final state without forming any narrow resonance structure in either K^+K^- or $K^\pm p$ system (non-resonant KKp). The background level was estimated from the yields below and above the ϕ -meson peak by using Monte Carlo simulations which were fitted to the angular distributions of K^+ , K^- and p in the real data. The Monte Carlo simulations reproduced the K^+K^- invariant mass (Fig. 1(c) and (d)) and K^-p invariant mass distributions in the real data. Although there is a kinematical overlap of $\Lambda(1520)$ and ϕ production in this energy range, the contamination of $\Lambda(1520)$ events in the final sample is suppressed in small $|t|$ regions. It was estimated as less than a few percent. The estimated systematic error on the cross section due to the background subtraction procedure was less than 0.8%.

The acceptance of the spectrometer was determined in Monte Carlo simulations using the GEANT3 simulation package [23]. Geometrical acceptance, resolution and efficiency of the detectors were taken into account. Since the acceptance depends on the input distributions, the simulations were iterated to reflect measured $d\sigma/dt$ and angular distributions, having started from flat distributions. The acceptance also depends on beam polarization and the mode of reconstruction. The validity of the acceptance calculation and the background subtraction was confirmed by checking the consistency of the cross section results among different reconstruction modes, and also by checking the consistency of the decay angular distributions obtained with different beam polarizations.

The differential cross sections were measured in terms of $t + |t|_{min}$ where $|t|_{min}$ is the minimum 4-momentum transfer from the incident photon to the ϕ -meson. Figure 2 shows the $d\sigma/dt$ in different photon energy regions. The $d\sigma/dt$ showed a forward peaking shape, suggesting the dominance of t-channel exchange processes. A fit to the $d\sigma/dt$ was performed with an exponential function; i.e. $(d\sigma/dt)_{t=-|t|_{min}} e^{b(t+|t|_{min})}$ with $(d\sigma/dt)_{t=-|t|_{min}}$ and b as free parameters. No strong energy dependence of the slope b was found beyond statistical errors. The average value of the slope b was $3.38 \pm 0.23 \text{ GeV}^{-2}$. When the average slope for data at all energies was used in the fit, the fitting curves described the data points well.

Figure 3 shows the energy dependence of $(d\sigma/dt)_{t=-|t|_{min}}$ when b is set to the average slope. The energy dependence of $(d\sigma/dt)_{t=-|t|_{min}}$ shows a non-monotonic behavior with a local maximum at $E_\gamma \sim 2 \text{ GeV}$. The local maximum is also seen using only the differential cross sections at the lowest $t + |t|_{min}$ bin where acceptance and signal-to-noise ratio is at a maximum. The local maximum still persisted when the analysis was repeated excluding events near the $\Lambda(1520)$ peak in K^-p system.

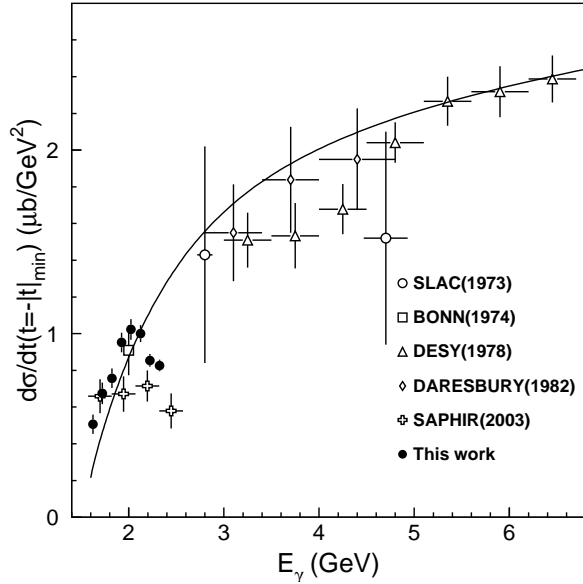


FIG. 3: Energy dependence of $(d\sigma/dt)_{t=-|t|_{min}}$. The closed circles are the results of the present work. Other data points are taken from Ref. [7, 8, 9, 10, 11, 12]. The error bars represent statistical errors. The systematic errors are discussed in the text. The solid curve represents the prediction of a model including the Pomeron trajectory, π and η exchange processes [15].

Data were compared with the prediction of a model including Pomeron exchange, π and η exchange processes [15]. A χ^2 test was performed to check whether the model prediction was statistically compatible. It gave $\chi^2 = 266$ for 8 degrees of freedom using the present measurements. The model is inconsistent with the present data points although it describes the data rather well at higher energies.

The decay angular distributions in the Gottfried-Jackson frame were obtained at forward angles ($-0.2 < t + |t|_{min} \leq 0$ GeV²) in two different energy-regions: (1) around the local maximum of the cross section ($\Delta E_1: 1.97 < E_\gamma < 2.17$ GeV) and (2) above the local maximum ($\Delta E_2: 2.17 < E_\gamma < 2.37$ GeV) where there are enough statistics and the acceptance is fairly flat over all angular variables.

Figure 4(a) shows the angular distribution $W(\cos\theta)$. In both energy regions, $W(\cos\theta)$ behaves as $\sim (3/4)\sin^2\theta$, indicating the dominance of helicity-conserving processes. A contribution from tensor-meson exchange, such as f'_2 -meson exchange, must be small since a contribution of this term would result in a deviation from the $\sin^2\theta$ form [15]. Note that this result is different from the measurement in a wider t range [12] which shows strong violation from $\sin^2\theta$ form. This may be understood by the production mechanism discussed in Ref. [20].

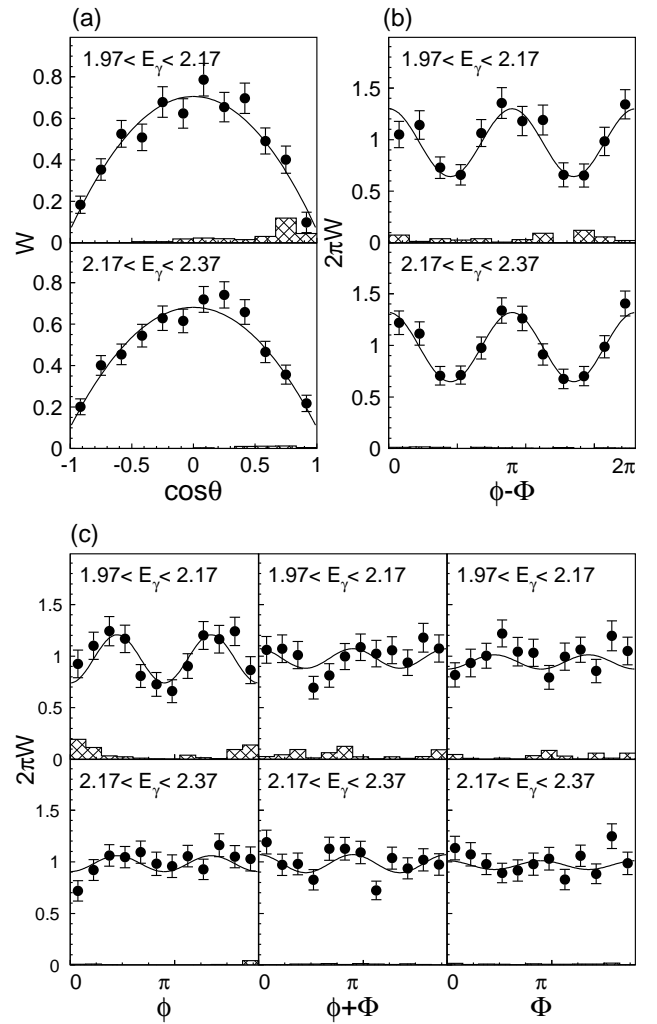


FIG. 4: Decay angular distributions for $-0.2 < t + |t|_{min}$ in the Gottfried-Jackson frame. The solid curves are the fit to the data. The hatched histograms are systematic errors.

Figure 4(b) shows the distribution $W(\phi-\Phi)$. We found $\bar{\rho}_{1-1}^1 = 0.189 \pm 0.024(\text{stat.}) \pm 0.006(\text{sys.})$ in ΔE_1 and $0.197 \pm 0.030(\text{stat.}) \pm 0.022(\text{sys.})$ in ΔE_2 . The positive value for $\bar{\rho}_{1-1}^1$ indicates that the contributions from natural parity exchange are bigger than those for unnatural parity exchange (π, η -meson exchange). The $\bar{\rho}_{1-1}^1$ is the same in the two energy regions within errors. This implies that the relative contribution of natural parity exchange and unnatural parity exchange remains constant in the two energy regions. Therefore, it is difficult to attribute the origin of the local maximum in the cross section to different strengths of the unnatural-parity exchange processes in the two energy regions.

Other one dimensional angular distributions $W(\phi)$, $W(\phi + \Phi)$ and $W(\Phi)$ are depicted in Fig. 4(c). No strong oscillation was found, except that the distribution $W(\phi)$ at ΔE_1 bin showed an oscillation ($\rho_{1-1}^0 = 0.120 \pm 0.027(\text{stat.}) \pm 0.011(\text{sys.})$). ρ_{1-1}^0 reflects the double

spin-flip transition from the incident photon to the outgoing ϕ -meson [18]. The spin-flip amplitudes are exactly zero in the case of pure scalar meson exchange and pseudoscalar meson exchange processes. The oscillation in the $W(\phi)$ distribution might be understood in the framework of a modified Donnachie-Landshoff Pomeron model motivated by the non-perturbative two-gluon-exchange dynamics [15]. However, this model fails to reproduce the non-monotonic energy dependence (see the solid curve in Fig. 3).

An alternative explanation might be the manifestation of a daughter Pomeron trajectory. In this case, the decay angular distributions may be similar to those for the Pomeron trajectory as observed, since contributions from both trajectories involve exchanges of natural-parity particles. While the decay angular distributions are useful to discriminate natural parity exchange from unnatural parity exchange, they are not useful to disentangle the two possible natural parity exchanges, i.e. Pomeron exchange and a daughter Pomeron exchange. On the other hand, the energy dependence of the cross sections is a good indicator for a daughter Pomeron exchange process. However, the fit suggested in Ref. [3] failed to predict the local maximum in the cross section with the proposed set of parameters.

In summary, the photoproduction of the ϕ -meson was studied for the first time by means of linearly polarized photons at forward angles in the low energy region from the threshold energy of $E_\gamma=1.57$ GeV to 2.37 GeV. The differential cross sections at $t = -|t|_{min}$ go non-monotonically as a function of E_γ , and show a local maximum at around 2.0 GeV. The polar angle distributions demonstrate dominance of helicity conserving processes and disfavor tensor f_2' meson exchange. The azimuthal angle distributions over the local maximum suggest that the local maximum is not due to additional unnatural-parity processes, but likely due to new dynamics which may involve a multi-gluon exchange beyond the Pomeron exchange process. Further theoretical and experimental studies are of great interest for clarifying photoproduction mechanisms in the low-energy region with the local maximum.

The authors thank the SPring-8 staff for supporting the BL33LEP beam line and the LEPS experiment. We thank H. Toki and A. Hosaka (RCNP) for fruitful discussions. This research was supported in part by the Ministry of Education, Science, Sports and Culture of Japan, by the National Science Council of Republic of China (Taiwan), Korea Research Foundation(KRF) Grant(2003-015-C00130) and National Science Foundation (NSF Award PHY-0244999).

-
- * Present address: Department of Physics and Astronomy, Ohio University, Athens, Ohio 45701
 - † Present address: Department of Physics, Kyoto University, Kyoto 606-8502, Japan
 - ‡ Present address: Laboratory of Nuclear Science, Tohoku University, Sendai, Miyagi 982-0826, Japan
 - § Present address: Center for Nuclear Study, University of Tokyo, 7-3-1 Hongo, Bunkyo, Tokyo 113-0033, Japan
 - ¶ Present address: Department of Applied Physics, National Defense Academy, Yokosuka 239-8686, Japan
 - ** Present address: Department of Physics, Tokyo Institute of Technology, Tokyo 152-8551, Japan
 - †† Present address: Department of Physics and Astronomy, Rice University, 6100 Main St. Houston MS 108, TX 77005-1892, USA
 - ‡‡ Present address: Department of Physics, Tohoku University, Sendai, Miyagi 980-8578, Japan
 - §§ Present address: Joint Institute for Nuclear Research, 141980, Dubna, Russia
 - ¶¶ Present address: Akita Research Institute of Brain and Blood Vessels, Akita 010-0874, Japan
 - *** Present address: Institute of Statistical Science, Academia Sinica, Nankang, 115 Taipei, Taiwan
 - ††† Present address: Illinois Institute of Technology, Chicago, Illinois 60616, USA
 - ‡‡‡ Present address: Research Center for Nuclear Physics, Osaka University, Ibaraki, Osaka 567-0047, Japan
 - §§§ Present address: National Superconducting Cyclotron Laboratory, Michigan State University, East Lansing, MI 48824-1321, USA
- [1] S. Donnachie, G. Dosch, P. Landshoff, and O. Nachtmann, *Pomeron Physics and QCD* (Cambridge University Press, 2002), reference therein.
 - [2] T. H. Bauer, R. D. Spital, D. R. Yennie, and F. M. Pipkin, *Rev. Mod. Phys.* **50**, 261 (1978).
 - [3] T. Nakano and H. Toki, in proceedings of International Workshop on Exciting Physics with New Accelerators Facilities, SPring-8, Hyogo (World Scientific) p. 48 (1997).
 - [4] A. I. Titov, T. S. H. Lee, H. Toki, and O. Streltsova, *Phys. Rev. C* **60**, 035205 (1999).
 - [5] L. S. Kisslinger and W.-H. Ma, *Phys. Lett. B* **485**, 367 (2000).
 - [6] F. J. Llanes-Estrada, S. R. Cotanch, P. J. de A. Bicudo, J. E. F. T. Ribeiro, and A. P. Szczepaniak, *Nucl. Phys. A* **710**, 45 (2002).
 - [7] J. Ballam *et al.*, *Phys. Rev. D* **7**, 3150 (1973).
 - [8] H. J. Besch *et al.*, *Nucl. Phys. B* **70**, 257 (1974).
 - [9] H. J. Behrend *et al.*, *Nucl. Phys. B* **144**, 22 (1978).
 - [10] D. P. Barber *et al.*, *Zeit. Phys. C* **12**, 1 (1982).
 - [11] E. Anciant *et al.*, *Phys. Rev. Lett.* **85**, 4682 (2000).
 - [12] J. Barth *et al.*, *Eur. Phys. J. A* **17**, 269 (2003).
 - [13] Y.-S. Oh and H. C. Bhang, *Phys. Rev. C* **64**, 055207 (2001).
 - [14] Q. Zhao, B. Saghai, and J. S. Al-Khalili, *Phys. Lett. B* **509**, 231 (2001).
 - [15] A. I. Titov and T.-S. H. Lee, *Phys. Rev. C* **67**, 065205 (2003).
 - [16] R. A. Williams, *Phys. Rev. C* **57**, 223 (1998).
 - [17] J. M. Laget, *Phys. Lett. B* **489**, 313 (2000).
 - [18] K. Schilling, P. Seyboth, and G. E. Wolf, *Nucl. Phys. B* **15**, 397 (1970).

- [19] M. Atkinson *et al.*, *Z. Phys.* **C27**, 233 (1985).
- [20] K. McCormick *et al.*, *Phys. Rev. C* **69**, 032203 (2004).
- [21] T. Nakano *et al.*, *Nucl. Phys. A* **684**, 71 (2001).
- [22] T. Ishikawa *et al.*, *Phys. Lett. B* **608**, 215 (2005).
- [23] R. Brun *et al.*, *CERN Program Library Long Writeup W5013*, CERN Applications Software Group (1993).